

An analytical-numerical method for calculating the stationary thermal field in electrical systems with elliptical cross-sections

Jerzy GOŁĘBIEWSKI and Marek ZARĘBA*

Faculty of Electrical Engineering, Białystok University of Technology, Wiejska 45D, 15-351 Białystok, Poland

Abstract. In this article, an analytical-numerical approach to calculating a stationary thermal field in the elliptical region is presented. The eigenfunctions of the Laplace operator were determined analytically, whereas the coefficients of the eigenfunctions were obtained numerically. The cooling was modeled with 3rd kind (Hankel's) boundary condition, where the total heat transfer coefficient was the sum of the convective and radiative components. The method was used to analyze the thermal field in an elliptical conductor and a dielectrically heated elliptical column. The basic parameters of these systems, i.e., their steady-state current rating and the maximum charge temperature, were determined. The results were verified using the finite element method and presented graphically.

Key words: analytical-numerical methods of field theory; elliptical conductors; Poisson's equation.

1. Introduction

The cross-sections of some electrical systems are elliptical, e.g., helically stranded non-magnetic conductors with elliptical [1–3], and semi-elliptical [4] cross-section. Elliptical homogeneous busbars are also used. In addition, models of cylindrical systems that deform to an elliptical shape have been discussed in the reference [5]. Regardless of this, elliptically shaped slots have been found in electrical machines [6, 7]. Some charges are heated by the dielectric method; these often take the form of an elliptical column.

One of the key parameters of the aforementioned systems is their temperature, e.g., it limits current that the conductor can carry (steady state current rating). Exceeding this value can threaten the thermal safety of the surroundings and lead to internal mechanical stresses; this can result in either minor or significant displacement of the wires. If shorting occurs, the resulting temperature may be so high that the delaminated wires will form a kind of “birdcage” in the conductor. In addition, the temperature of the dielectrically heated charge should not exceed the permitted value. Above this threshold, the charge may lose its desirable properties or become damaged. The difference between the maximum and the minimum charge temperatures, i.e., the gradient, is also important. For the reasons that have been set out, the thermal field analysis in electrical systems is an important technical task that should be undertaken.

The analytical-numerical method, which is covered in this article, has certain advantages; one of these is the possibility of calculating the thermal field at any point of an area that is bounded by an ellipse. Using numerical methods [8–10], the

field is only determined in the nodes of the grid, i.e., in selected points only. This means there is a finite number of degrees of freedom for the numerical solutions.

On the other hand, analytical solutions for elliptical boundaries [11–14] only apply to first and second kind boundary conditions, i.e., the Dirichlet or Neumann boundary conditions. The proposed analytical-numerical method also allows modeling of heat transfer in elliptical configurations, with the use of third kind boundary conditions, e.g., Hankel's:

$$\left(\frac{dT}{dn}\right)_P = BT|_P \quad (1)$$

where the left-hand side of the equation is the derivative of the temperature, T , with respect to the external normal at the point P on the boundary's surface, when $B = const$.

Despite an intensive search, the authors of this paper could not find any analytical-numerical calculations for elliptical-cylindrical coordinates in the professional literature. For this reason, the given bibliography has been limited to those previously cited analytical or numerical solutions in the elliptical regions. The authors believe that the analytical-numerical method presented in this paper has filled the gap in the subject being discussed. Moreover, in contrast to the numerical methods, the analytical-numerical method means that the field at an arbitrary point in the system can be determined. When compared with the analytical methods, the progress that has been made is modeling with the use of third kind (Hankel's) boundary conditions.

2. A boundary problem for the thermal field in an area bounded by an ellipse

Figure 1 shows the area bounded by an ellipse, where the semi-major axis and the semi-minor axis have been denoted as a and b , respectively. The perimeter of the ellipse is defined by

*e-mail: m.zareba@pb.edu.pl

Manuscript submitted 2020-09-24, revised 2020-12-17, initially accepted for publication 2020-12-17, published in April 2021

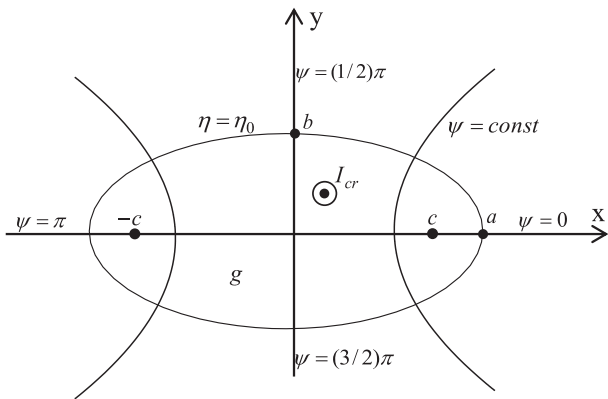


Fig. 1. The area bounded by an ellipse and heated by an internal heat source with efficiency g

the coordinate $\eta = \eta_0$, whereas c is the abscissa of the focal point. The thermal field $T(\eta, \psi)$ of the area is generated by an internal heat source with efficiency g .

In Section 4, simplifying assumptions will be given. These assumptions will create a physical model of the examined electrical systems.

The boundary problem of the 2D model was defined with respect to the temperature increment $v(\eta, \psi) = T(\eta, \psi) - T_a$, where $v(\eta, \psi)$ are the elliptical-cylindrical coordinates (Fig. 1), whereas T_a is the ambient temperature. The stationary distribution of the temperature increment in the system is described by Poisson's equation [15–17]:

$$\frac{1}{c^2 (\cosh^2 \eta - \cos^2 \psi)} \left(\frac{\partial^2 v(\eta, \psi)}{\partial \eta^2} + \frac{\partial^2 v(\eta, \psi)}{\partial \psi^2} \right) = -\frac{g}{\lambda} \quad (2)$$

for $0 \leq \eta \leq \eta_0$, $0 \leq \psi \leq 2\pi$, where λ is the equivalent thermal conductivity.

It was assumed that the surface $\eta = \eta_0$ emits heat to the atmosphere according to Newton's law. The aforementioned energy transfer is described by third kind (Hankel's) boundary condition [15, 17], which, for elliptical-cylindrical coordinates, takes the form:

$$\lambda [\text{grad } v(\eta, \psi)] \cdot \vec{1}_\eta \Big|_{\eta=\eta_0} = -\alpha \cdot v(\eta = \eta_0, \psi), \quad (3a)$$

for $0 \leq \psi \leq 2\pi$, which leads to:

$$\frac{1}{c \sqrt{\cosh^2 \eta - \cos^2 \psi}} \frac{\partial v(\eta, \psi)}{\partial \eta} \Big|_{\eta=\eta_0} = -\frac{\alpha}{\lambda} \cdot v(\eta = \eta_0, \psi) \quad (3b)$$

for $0 \leq \psi \leq 2\pi$, where α , is the total heat transfer coefficient, taking convection and radiation into account.

Equations (2) and (3) define the boundary problem for the thermal field distribution. To the best of the authors' knowledge, both the analytical and the analytical-numerical solution of Eq. (2) with the boundary condition (3b) have not been published in the professional literature.

3. The solution to the boundary problem of a thermal field in an ellipse

The solution to the problem (2)–(3b) that is being sought, consists of a particular integral of a heterogeneous equation, i.e., Poisson (2) and a general integral of a homogeneous equation, i.e., Laplace; this can be obtained by setting the right side of Eq. (2) to zero [18]. This particular integral was calculated on the basis of the reference [16] (the case of function of η, ψ variables in elliptic coordinates). On the other hand, the general integral was calculated using the separation of variables method [17, 19]. The superposition of the aforementioned integrals leads to the following solution:

$$v(\eta, \psi) = -\frac{gc^2}{8\lambda} [\cosh(2\eta) + \cos(2\psi)] + (A_0 + B_0\eta)(C_0 + D_0\psi) + \sum_{n=1}^{\infty} [A_n \cosh(n\eta) + B_n \sinh(n\eta)] \cdot [C_n \cos(n\psi) + D_n \sin(n\psi)] \quad (4)$$

for $0 \leq \eta \leq \eta_0$, $0 \leq \psi \leq 2\pi$.

It follows from the system's configuration (Fig. 1), that the solution with respect to the coordinate ψ must be periodic and even, which results in $D_0 = D_n = 0$. The singular and non-physical terms must also be removed. The heat flux ($\vec{q} = -\lambda \cdot \text{grad } v(\eta, \psi)$) in a singular point (focus) must be finite. After the application of Eq. (4) to calculate the flux limits \vec{q} in focus ($\eta = 0, \psi = 0$), the functions η and $\sinh(n\eta)$ were rejected ($B_0 = B_n = 0$ was accepted). The inclusion of the above conclusions and the introduction of new constants resulted in the solution with the following form:

$$v(\eta, \psi) = -\frac{gc^2}{8\lambda} [\cosh(2\eta) + \cos(2\psi)] + F_0 + \sum_{n=1}^N F_n \cosh(n\eta) \cos(n\psi) \quad (5)$$

for $0 \leq \eta \leq \eta_0$, $0 \leq \psi \leq 2\pi$,

The unknown coefficients F_0 and F_n were calculated using Hankel's boundary condition (3b) (third kind). In order to achieve this, the sum of the series (5) was limited to a finite number with N terms and substituted into (3b), resulted in the following:

$$\frac{1}{c \sqrt{\cosh^2(\eta_0) - \cos^2(\psi)}} \left[-\frac{gc^2}{4\lambda} \sinh(2\eta_0) + \sum_{n=1}^N n F_n \sinh(n\eta_0) \cos(n\psi) \right] = -\frac{\alpha}{\lambda} \left[-\frac{gc^2}{8\lambda} [\cosh(2\eta_0) + \cos(2\psi)] + F_0 + \sum_{n=1}^N F_n \cosh(n\eta_0) \cos(n\psi) \right] \quad (6)$$

for $0 \leq \psi \leq 2\pi$.

Equation (6) was then multiplied by $\cos(m\psi)$ and each side was integrated separately with respect to the angular coordinate ψ in the range $\langle 0, 2\pi \rangle$; this then led to Eq. (7a) where $m = 1, 2, \dots, N$. The next Eq. (7b) was obtained by integrating each side of Eq. (6) separately, with respect to the angular coordinate ψ in the range $\langle 0, 2\pi \rangle$. As a result, the Eqs. (7a) and (7b) form a system for $N+1$ of the equations with respect to the unknowns F_0, \dots, F_n :

$$\sum_{n=1}^N F_n I_1(m, n) = I_2(m) \quad \text{for } m = 1, 2, \dots, N, \quad (7a)$$

$$\sum_{n=1}^N F_n I_3(n) + F_0 \cdot \frac{2\pi\alpha}{\lambda} = I_4 \quad (7b)$$

where:

$$I_1(m, n) = \begin{cases} \frac{n \sinh(n\eta_0)}{c} \cdot \int_0^{2\pi} \frac{\cos(n\psi) \cos(m\psi) d\psi}{\sqrt{\cosh^2(\eta_0) - \cos^2(\psi)}} & \text{for } m \neq n, \\ \frac{m \sinh(m\eta_0)}{c} \cdot \int_0^{2\pi} \frac{\cos^2(m\psi) d\psi}{\sqrt{\cosh^2(\eta_0) - \cos^2(\psi)}} + \frac{\alpha \pi \cosh(m\eta_0)}{\lambda} & \text{for } m = n, \end{cases} \quad (8a)$$

$$I_2(m) = \begin{cases} \frac{gc \sinh(2\eta_0)}{4\lambda} \cdot \int_0^{2\pi} \frac{\cos(m\psi) d\psi}{\sqrt{\cosh^2(\eta_0) - \cos^2(\psi)}} & \text{for } m \neq 2, \\ \frac{gc \sinh(2\eta_0)}{4\lambda} \cdot \int_0^{2\pi} \frac{\cos(2\psi) d\psi}{\sqrt{\cosh^2(\eta_0) - \cos^2(\psi)}} + \frac{\pi gc^2 \alpha}{8\lambda^2} & \text{for } m = 2, \end{cases} \quad (8b)$$

$$I_3(n) = \frac{n \sinh(n\eta_0)}{c} \cdot \int_0^{2\pi} \frac{\cos(n\psi) d\psi}{\sqrt{\cosh^2(\eta_0) - \cos^2(\psi)}}, \quad (8c)$$

$$I_4 = \frac{gc \sinh(2\eta_0)}{4\lambda} \cdot \int_0^{2\pi} \frac{d\psi}{\sqrt{\cosh^2(\eta_0) - \cos^2(\psi)}} + \frac{\pi gc^2 \alpha}{4\lambda^2} \cosh(2\eta_0). \quad (8d)$$

The integrals in Eqs. (8a)–(8d) can be identified as complete elliptic integrals of the first kind [20]. However, transforming Eqs. (8a)–(8d) to the form presented in the reference [20] is very arduous. It is considerably easier to directly calculate integrals (8a)–(8d) using an arbitrary method of numerical integration [21]. After determining the integrals in Eqs. (8a)–(8d), it is necessary to numerically solve the system of Eqs. (7a)–(7b)

for the unknown coefficients F_n and the constant F_0 in Eq. (5); this solves the boundary problem (2)–(3b). According to the definition of the increment $\nu(\eta, \psi)$, the final field distribution in the system could then be obtained by inserting the ambient temperature T_a into the right side of Eq. (5).

4. Applications

The first example of an application for this method is the analysis of a thermal field in a non-magnetic conductor with an elliptical cross-section (Fig. 1). The conductor is made of helically stranded bundles of aluminum wire, with a total (effective) cross-section $S < \pi ab$. The air that fills the gaps between the bundles reduces the thermal conductivity of the system compared to solid aluminum. The length of the conductor is much greater than the major axis of the ellipse; this means that the system can be treated as two-dimensional. The conductor was laid horizontally in a closed space (in-door conditions). For this reason, the effect of solar radiation could be neglected and a constant ambient temperature T_a was assumed. A constant value of the total heat transfer α was adopted for the perimeter of the ellipse.

Taking the above assumptions into consideration, the increment of the stationary temperature field (with respect to T_a) could be described by the two-dimensional Poisson Eq. (2). The efficiency of the heat source g on the right-hand side of Eq. (2) is related to the electrical current flowing through the conductor at the mains frequency

$$g = \frac{P}{V} = \frac{k_s k_n R_{DC} |I|^2}{\pi a b l} = k_s k_n \rho \frac{|I|^2}{S \cdot \pi a b}, \quad (9)$$

where: P corresponds to the power losses that result from the flow of alternating current with the root mean square value $|I|$, V is the volume of a segment of the conductor with length l , R_{DC} is the DC resistance, k_s is the skin factor [1], k_n is the stranding factor [22], which takes the helical twisting of the wires into account, $\rho(T_{\max})$ is the resistivity of the conductor at its maximum operating temperature and S is the sum of the cross-sections of the bundles (the twisted aluminum wires). The following data values were used for the calculations:

$$\begin{aligned} b &= 0.00690988 \text{ m}, \quad a = 2b, \quad \lambda_1 = 180 \text{ W}/(\text{mK}), \\ T_{\max} &= 70^\circ\text{C}, \quad T_a = 25^\circ\text{C}, \quad T_{\text{max}} = 70^\circ\text{C}, \\ k_s &= 1.02, \quad k_n = 1.02, \\ \rho &= 2.88335 \cdot 10^{-8} \Omega \cdot \text{m}, \\ S &= 270 \text{ mm}^2, \quad \alpha = 16 \text{ W}/(\text{mK}). \end{aligned} \quad (10)$$

The values above also determined the secondary parameters that are essential for the analysis of the elliptical system, which are: the abscissa of the focus of the ellipse $c = \sqrt{a^2 - b^2}$ and the equation of its perimeter $\eta_0 = \text{arc}[\sinh(b/c)]$.

Based on the method presented earlier (Sec. 3), a computer program was written in the Mathematica 11.1 environment [21]. The program then was used to numerically solve the integrals

(8a)–(8d), as well as the system of Eqs. (7a)–(7b). For this purpose, the iterative Krylov method was used. The program was then used to calculate the sum of the ambient temperature T_a and the series (5). The program also visualized the results. While calculating an infinite series from Eq. (5), it was found that it was strongly convergent. The addition of more than 12 terms resulted in a change in the calculation at the sixth decimal place at any point in the system; for this reason, the calculation of the series from Eq. (5) was limited to the first 12 terms.

An important parameter of a conductor is the steady state current rating I_{cr} ; this is limited by the maximum temperature T_{max} the conductor can be heated to during sustained operation. Thus, the maximum value of the current I_{cr} must be found, to ensure that the highest temperature at the conductor's surface does not exceed T_{max} . The parameter T_{max} exists to ensure the thermal safety of the surroundings. Among all of the points on the perimeter of the elliptical conductor, its upper and lower co-vertices are the closest to the center (Fig. 1); for this reason, they are the hottest points of the boundary. Therefore, the steady-state current rating of the conductor can be determined from the Eq. (11)

$$T\left(\eta = \eta_0, \psi = \frac{\pi}{2}, I_{cr}\right) = T_{max}. \quad (11)$$

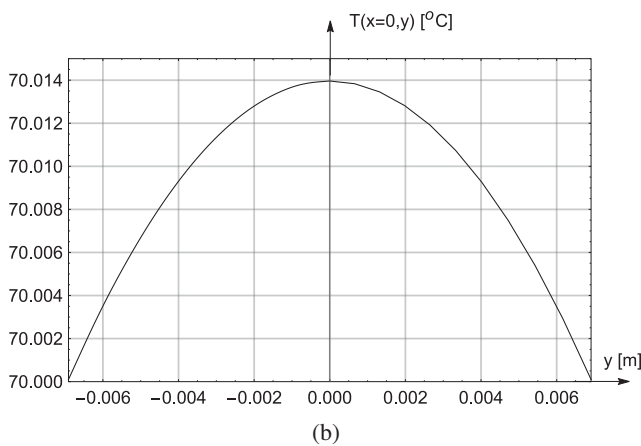
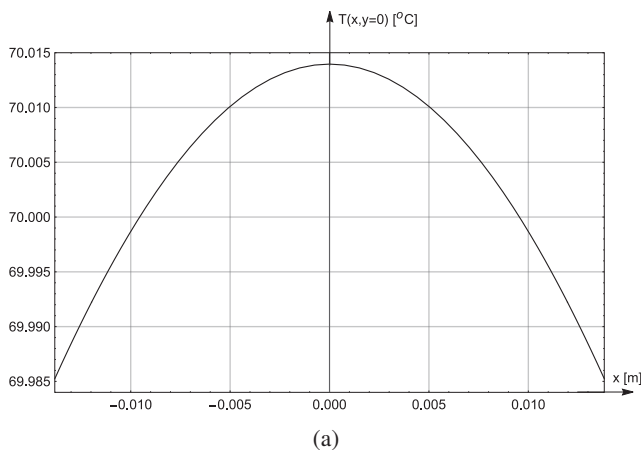


Fig. 2. (a) The temperature distribution on the major axis ($y = 0$) of the elliptical conductor with an electrical load of $I_{cr} = 658.6$ A (b) The temperature distribution on the minor axis ($x = 0$) of the elliptical conductor with an electrical load of $I_{cr} = 658.6$ A

Equation (11) was then solved iteratively in the Mathematica 11.1 software [21] using a While loop; for the data from set (10), the result $I_{cr} = 658.6$ A was obtained. Following this, the thermal field for the above stated current was determined for an elliptical conductor. For the sake of convenience, the selected distributions were presented in Cartesian coordinates, $x = c \cosh \eta \cos \psi$ and $y = c \sinh \eta \sin \psi$. Figures 2a and 2b illustrate the temperature change on the major ($y = 0$, Fig. 2a) and minor ($x = 0$, Fig. 2b) axes, respectively. In turn, Fig. 3 shows the isotherms of the temperature field in the conductor; due to the high thermal conductivity of aluminum, the temperature distribution (Figs. 2a and 2b and Fig. 3) was nearly uniform throughout the entire volume of the conductor.

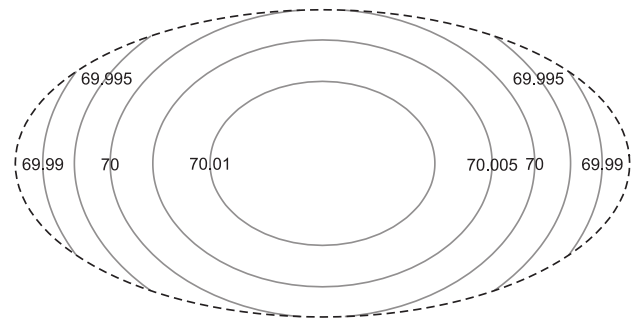


Fig. 3. The isotherms of the temperature field in the cross-section of the elliptical conductor with an electrical load of $I_{cr} = 658.6$ A where $\lambda_1 = 180$ W/(mK)

The second example is the analysis of the temperature field in a long column with an elliptical base; its cross-section is illustrated in Fig. 4. The dielectric column (charge) is heated electronically and every point in this block is a heat source with an efficiency g . The condition $g = const$ is well met when one electrode of the capacitor is grounded (Fig. 4). At the same time, the maximum difference in the potential on the second electrode should not exceed 10%. The above conditions can be satisfied by powering the capacitor at multiple points or by introducing coils at suitable points between the electrodes [23].

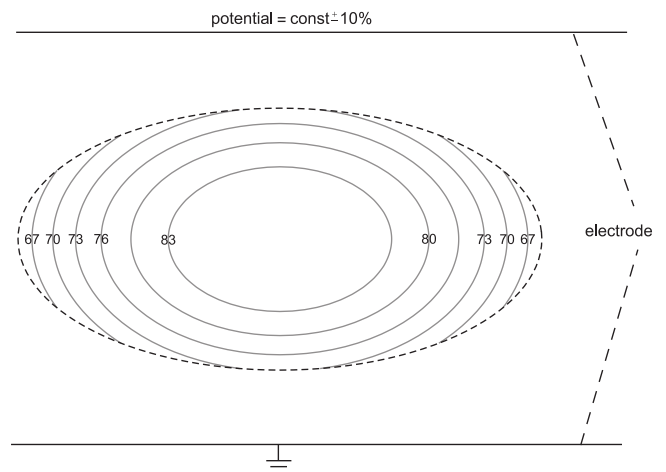


Fig. 4. The isotherms of the temperature field in the cross-section of long dielectric column where $\lambda_2 = 0.2$ W/(mK)

For the sake of comparison, as in the previous example, the same efficiency g was assumed; for the same reason, the parameters (10) were unchanged, except for λ . In this example, it was assumed that $\lambda_2 = 0.2 \text{ W/(mK)}$. Figure 4 shows the isotherms of the temperature field for the above test example.

The scope of the application of Poisson's equation in technology and physics is very broad. Apart from the temperature inside a system with a continuous heat generation, Poisson's equation describes the distribution field of the velocities of a fluid flowing from the source. The Poisson's equation also describes the potentials of other physical fields; these are electrostatic potential in the presence of electrical charges and gravitational potential in the presence of a field sources (mass).

5. Numerical verification of the method

The presented method was then verified; the obtained results were then compared with the numerical calculations [24] and [25]. For this reason, the temperature problem in Eqs. (2) and (3) was solved again using the finite element method [24–27] in

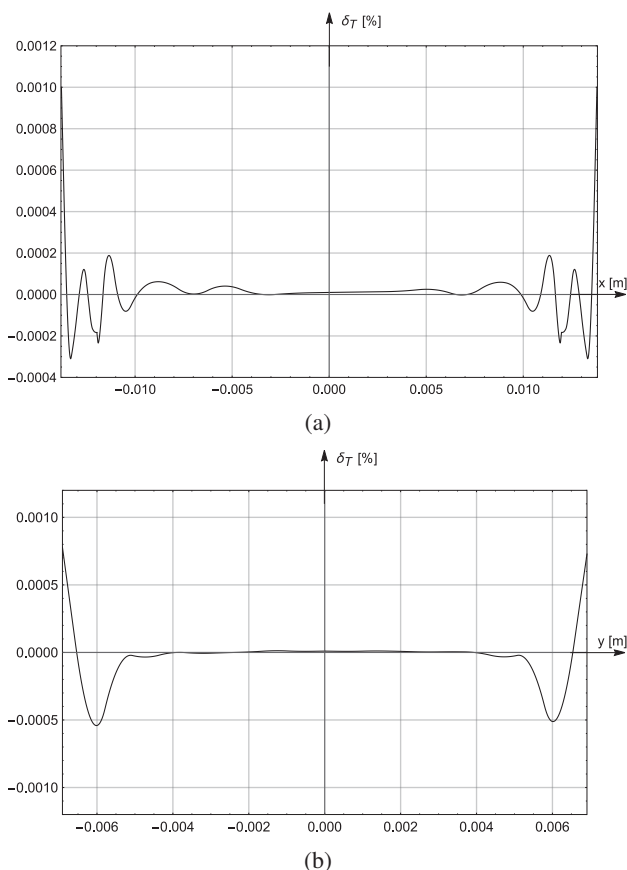


Fig. 5. (a) The relative differences from Eq. (12) between the results of the analytical-numerical method and the finite element method for $y = 0$ (the major axis of the ellipse) where $\lambda_2 = 0.2 \text{ W/(mK)}$ (dielectric) (b) The relative differences from Eq. (12) between the results of the analytical-numerical method and the finite element method for $x = 0$ (the minor axis of the ellipse) where $\lambda_2 = 0.2 \text{ W/(mK)}$ (dielectric)

the Mathematica software [21]. Then, the relative difference in the temperature increment was calculated using the following formula:

$$\delta_T = 100\% \frac{[T(x,y) - T_a] - [T_{FE}(x,y) - T_a]}{T(x,y) - T_a} \quad (12)$$

where, $T(x,y)$ is the temperature distribution obtained from the presented analytical-numerical method and $T_{FE}(x,y)$ is the temperature distribution calculated from the finite element method. Figures 5a and 5b illustrate Eq. (12) for the case of the dielectric column ($\lambda_2 = 0.2 \text{ W/(mK)}$) on the major ($y = 0$, Fig. 5a) and the minor ($x = 0$, Fig. 5b) axes of the ellipse, respectively. The relative differences from Eq. (12) in the elliptical conductor ($\lambda_1 = 180 \text{ W/(mK)}$) where about three times smaller than presented in Figs. 5a and 5b.

6. Final remarks

- A. This article describes a novel analytical-numerical approach to determining a stationary thermal field in the elliptical region. Cooling the system was modeled using third kind boundary condition (Hankel's) (3b). The total heat transfer coefficient takes into account both the convective and radiative energy transfer. The eigenfunctions of the Laplace operator (5) were established analytically from the superposition of the general and particular integral of the Poisson's Eq. (2) and by the separation of variables method. The coefficients of the eigenfunctions were determined numerically from the system of Eqs. (7a and 7b) after the elliptical integrals (8a–8d) had been calculated.
- B. The thermal conductivity λ has a considerable influence on the distribution of the temperature field. When the value of λ_2 is low, heat dissipation to the outside of the system is difficulted; this results in a higher temperature for the same efficiency of the sources g . For example, in the center of the ellipse, $T(\eta = 0, \psi = \pi/2, \lambda_2) = 87.32^\circ\text{C} > T(\eta = 0, \psi = \pi/2, \lambda_1) = 70.014^\circ\text{C}$. The area with a temperature higher than 70°C was substantially larger as well, as judged from Fig. 4, with respect to Fig. 3. Additionally, a lower value of λ_2 definitely increased the drop in the temperature gradient, e.g., the difference in the center and right vertice of the ellipse was equal to

$$[T(\eta=0, \psi=\pi/2, \lambda_2) - T(\eta=\eta_0, \psi=0, \lambda_2)] = 22.42^\circ\text{C} > [T(\eta=0, \psi=\pi/2, \lambda_1) - T(\eta=\eta_0, \psi=0, \lambda_1)] = 0.029^\circ\text{C}.$$

As has been shown, a high value of λ_1 nearly evens out the temperature distribution in the system.

It follows from Figs. 3 and 4 that the perimeter of the system (the dashed line) is never isothermal. A suitable temperature at the higher and lower co-vertices of the ellipse is always larger than in the right and left vertices. This is a result of the different distances from those points to the center ($b < a$). For this reason, the isotherms do not have a common focus with the perimeter of the system.

- C. It follows from Figs. 5a and 5b, that the relative differences (12) in the temperature distributions, calculated using the analytical-numerical method and the finite element method, are very small. Therefore, the developed method leads to nearly equivalent results as the widely applied numerical method.
- D. In the special one-dimensional case ($a = b$), the abscissa of the focus $c = \sqrt{a^2 - b^2}$ is zero. As a result of the above, singularities will occur in the calculation. In addition, it should be noted that the cylindrical (polar) coordinate system is not a special case of the elliptical coordinate system. This is proved by Lamé's coefficients (metrics) of both systems [16]. So, the condition of the applicability of the presented method is maintain the two-dimensionality, or $a \neq b$.

Acknowledgements. The paper was prepared in Technical University of Białystok within a framework of the project WZ/WE-IA/2/2020 sponsored by the Ministry of Science and Higher Education.

REFERENCES

- [1] V.T. Morgan, "The current distribution, resistance and internal inductance of linear power system conductors – a review of explicit equations", *IEEE Trans. Power Deliv.* 28(3), 1252–1262 (2013).
- [2] R. Suchtanke, *Alternating current loss measurement of power cable conductors with large cross sections using electrical methods*, Doctoral dissertation, Technischen Universität, Berlin, 2008.
- [3] R. Sikora, J. Purczyński, and W. Lipiński, "Das magnetische Feld des gleich-stromdurchflossenen Leiters von elliptischen Querschnitt", *Arch. Elektrotechnik* 55, 223–226 (1973).
- [4] Prasanna Shinde, Jitendra Shukla, and E. Rajkumar, "Busbar profile optimization using finite element analysis", *Int. J. Mech. Prod. Eng.* 6(2), 30–32 (2018).
- [5] J. Purczyński and R. Sikora, "Application of the Ritz method to calculate the capacity" (in Polish), *Arch. Electr. Eng.* 22, 611–619 (1973).
- [6] W. Peterson, "Calculation of the impedance of a conductor with an elliptic cross-section in the slot of an electric machine", *Arch. Elektrotechnik* 60, 63–68 (1978).
- [7] W. Peterson, "Electrodynamic forces acting on a conductor with elliptic cross-section in the slot of an electric machine", *Arch. Elektrotechnik* 63, 135–139 (1981).
- [8] Z.-C. Li, L.-P. Zhang, Y. Wei, M.-G. Lee, and J.Y. Chiang, "Boundary methods for Dirichlet problems of Laplace's equation in elliptic domains with elliptic holes", *Eng. Anal. Bound. Elem.* 61, 91–103 (2015).
- [9] L.-P. Zhang, Zi.-C. Li, and M.-G. Lee, "Boundary methods for mixed boundary problems of Laplace's equation in elliptic domains with elliptic holes", *Eng. Anal. Bound. Elem.* 63, 92–104 (2016).
- [10] P. Rolicz, "Eddy currents in an elliptic conductor by a transverse alternating magnetic field", *Arch. Elektrotechnik* 68, 423–431 (1985).
- [11] H. Ragueb, "An analytical study of the periodic laminar forced convection of non-Newtonian nanofluid flow inside an elliptical duct", *Int. J. Heat Mass Transf.* 127, 469–483 (2018).
- [12] M. Benmerkhi, M. Afrid, and D. Groulx, "Thermally developing forced convection in a metal foam-filled elliptic annulus", *Int. J. Heat Mass Transf.* 97, 253–269 (2016).
- [13] F.M. Mahfouz, "Heat conduction within an elliptic annulus heated at either CWT or CHF", *Appl. Math. Comput.* 266, 357–368 (2015).
- [14] W. Piguang, Z. Mi, and D. Xiuli, "Analytical solution and simplified formula for earthquake induced hydrodynamic pressure on elliptical hollow cylinders in water", *Ocean Eng.* 148, 149–160 (2018).
- [15] M.N. Ozisik, *Heat Conduction*, John Wiley & Sons, New York, 1980.
- [16] P. Moon and D.E. Spencer, *Field theory for engineers*, D. Van Nostrand Company, Inc., Princeton, New York, 1961.
- [17] M.J. Latif, *Heat conduction*, Springer-Verlag, Haidelberg, 2009.
- [18] L.C. Evans, *Partial differential equations*, American Mathematical Society Providence, Rhode Islands, 2010.
- [19] D.W. Hahn and M.N. Ozisik, *Heat Conduction*, John Wiley & Sons, New Jersey, 2012.
- [20] A. Abramowitz and I.A. Stegun, *Handbook of mathematical functions with formulas, graphs, and mathematical tables*, Dover Publications, Inc., New York, 1972.
- [21] Wolfram Research, Inc., *Mathematica*, Illinois: Wolfram Research Inc., 2018.
- [22] G.J. Anders, *Rating of electric power cables: ampacity computations for transmission, distribution, and industrial applications*, McGraw-Hill Professional, New York, 1997.
- [23] M. Hering, *Fundamentals of electroheat (part 2)*, Wydawnictwo Naukowo-Techniczne, Warsaw, 1998, [in Polish].
- [24] P. Nithiarasu, R.W. Lewis, and K.N. Seetharamu, *Fundamentals of the finite element method for heat and mass transfer*, John Wiley & Sons, 2016.
- [25] A. Steckiewicz, J.M. Stankiewicz, and A. Choroszucho, "Numerical and circuit modeling of the low-power periodic WPT systems", *Energies* 13(10), 1–17 (2020).
- [26] S. Brenner and R.L. Scott, *The mathematical theory of finite element methods*, Springer, Berlin, 2008.
- [27] S. Berhausen and S. Paszek, "Use of the finite element method for parameter estimation of the circuit model of a high power synchronous generator", *Bull. Pol. Acad. Sci. Tech. Sci.* 63(3), 575–582 (2015).